Effects of Firing Synchrony on Signal Propagation in Layered Networks

G. T. Kenyon,[1] E. E. Fetz,[2] R. D. Puff[1]
[1]Department of Physics FM-15, [2]Department of Physiology and Biophysics SJ-40
University of Washington, Seattle, Wa. 98195

ABSTRACT

Spiking neurons which integrate to threshold and fire were used to study the transmission of frequency modulated (FM) signals through layered networks. Firing correlations between cells in the input layer were found to modulate the transmission of FM signals under certain dynamical conditions. A tonic level of activity was maintained by providing each cell with a source of Poisson-distributed synaptic input. When the average membrane depolarization produced by the synaptic input was sufficiently below threshold, the firing correlations between cells in the input layer could greatly amplify the signal present in subsequent layers. When the depolarization was sufficiently close to threshold, however, the firing synchrony between cells in the initial layers could no longer effect the propagation of FM signals. In this latter case, integrate-and-fire neurons could be effectively modeled by simpler analog elements governed by a linear input-output relation.

1 Introduction

Physiologists have long recognized that neurons may code information in their instantaneous firing rates. Analog neuron models have been proposed which assume that a single function (usually identified with the firing rate) is sufficient to characterize the output state of a cell. We investigate whether biological neurons may use firing correlations as an additional method of coding information. Specifically, we use computer simulations of integrate-and-fire neurons to examine how various levels of synchronous firing activity affect the transmission of frequency-modulated

(FM) signals through layered networks. Our principal observation is that for certain dynamical modes of activity, a sufficient level of firing synchrony can considerably amplify the conduction of FM signals. This work is partly motivated by recent experimental results obtained from primary visual cortex [1, 2] which report the existence of synchronized stimulus-evoked oscillations (*SEO's*) between populations of cells whose receptive fields share some attribute.

2 Description of Simulation

For these simulations we used integrate-and-fire neurons as a reasonable compromise between biological accuracy and mathematical convenience. The subthreshold membrane potential of each cell is governed by an over-damped second-order differential equation with source terms to account for synaptic input:

$$\left(\tau_r \frac{\partial^2}{\partial t^2} + \frac{\partial}{\partial t} + \frac{1}{\tau_d}\right) \phi_k = \sum_{j=1}^{N} \sum_{t'_j} T_{kj} \delta(t - t'_j) + \sum_{p_k} T_P \delta(t - p_k) \qquad (1)$$

where ϕ_k is the membrane potential of cell k, N is the number of cells, T_{kj} is the synaptic weight from cell j to cell k, t'_j are the firing times for the j^{th} cell, T_P is the synaptic weight of the Poisson-distributed input source, p_k are the firing times of Poisson-distributed input, and τ_r and τ_d are the rise and decay times of the *EPSP*. The Poisson-distributed input represents the synaptic drive from a large presynaptic population of neurons.

Equation 1 is augmented by a threshold firing condition

$$\text{if} \quad \begin{cases} \phi_k(t) = \theta(t - t'_k) \\ \dot{\phi}_k(t) > 0 \\ t - t'_k > \tau_a \end{cases} \qquad \text{then} \quad \begin{cases} \phi_k(t + 0^+) = \phi_r \\ \dot{\phi}_k(t + 0^+) = \dot{\phi}_r \end{cases} \qquad (2)$$

where $\theta(t - t'_k)$ is the threshold of the k^{th} cell, and τ_a is the absolute refractory period. If the conditions (2) do not hold then ϕ_k continues to be governed by equation 1.

The threshold is ∞ during the absolute refractory period and decays exponentially during the relative refractory period:

$$\theta(t - t'_k) = \begin{cases} \infty, & \text{if } t - t'_k < \tau_a; \\ \theta_p e^{-(t - t'_k)/\tau_p} + \theta_0, & \text{otherwise,} \end{cases} \qquad (3)$$

where, θ_0 is the resting threshold value, θ_p is the maximum increase of θ during the relative refractory period, and τ_p is the time constant characterizing the relative refractory period.

2.1 Simulation Parameters

τ_r and τ_d are set to 0.2 msec and 1 msec, respectively. T_P and T_{kj} are always $(1/100)\theta_0$. This strength was chosen as typical of synapses in the CNS. To sustain

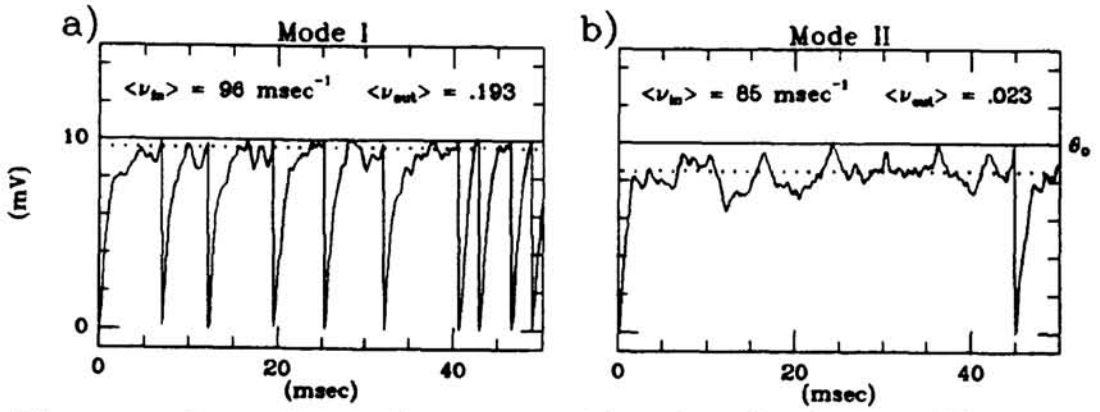

Figure 1: Example membrane potential trajectories for two different modes of activity. *EPSP's* arrive at mean frequency, ν_{in}, that is higher for mode I (a) than for mode II (b). Dotted line below threshold indicates asymptotic membrane potential.

activity, during each interval τ_d, a cell must receive $\approx (\theta_0/T_P) = 100$ Poisson-distributed inputs. Resting potential is set to 0.0 mV and θ_0 to 10 mV. ϕ_r and $\dot{\phi}_r$ are set to 0.0 mV and -1.0 mV/msec, which simulates a small hyperpolarization after firing. τ_a and τ_p were each set to 1 msec, and θ_p to 1.0 mV.

3 Response Properties of Single Cells

Figure 1 illustrates membrane potential trajectories for two modes of activity. In mode I (fig. 1a), synaptic input drives the membrane potential to an asymptotic value (dotted line) within one standard deviation of θ_0. In mode II (fig. 1b), the asymptotic membrane potential is more than one standard deviation below θ_0.

Figure 2 illustrates the change in average firing rate produced by an *EPSP*, as measured by a cross-correlation histogram (*CCH*) between the Poisson source and the target cell. In mode I (fig. 2a), the *CCH* is characterized by a primary peak followed by a period of reduced activity. The derivative of the *EPSP*, when measured in units of θ_0, approximates the peak magnitude of the *CCH*. In mode II (fig. 2b), the *CCH* peak is not followed by a period of reduced activity. The *EPSP* itself, measured in units of θ_0 and divided by τ_d, predicts the peak magnitude of the *CCH*. The transform between the *EPSP* and the resulting change in firing rate has been discussed by several authors [3, 4]. Figures 2c and 2d show the cumulative area (*CUSUM*) between the *CCH* and the baseline firing rate. The *CUSUM* asymptotes to a finite value, Δ, which can be interpreted as the average number of additional firings produced by the *EPSP*.

Δ increases with *EPSP* amplitude in a manner which depends on the mode of activity (fig. 2e). In mode II, the response is amplified for large inputs (concave up). In mode I, the response curve is concave down. The amplified response to large inputs during mode II activity is understandable in terms of the threshold crossing mechanism. Populations of such cells should respond preferentially to synchronous synaptic input [5].

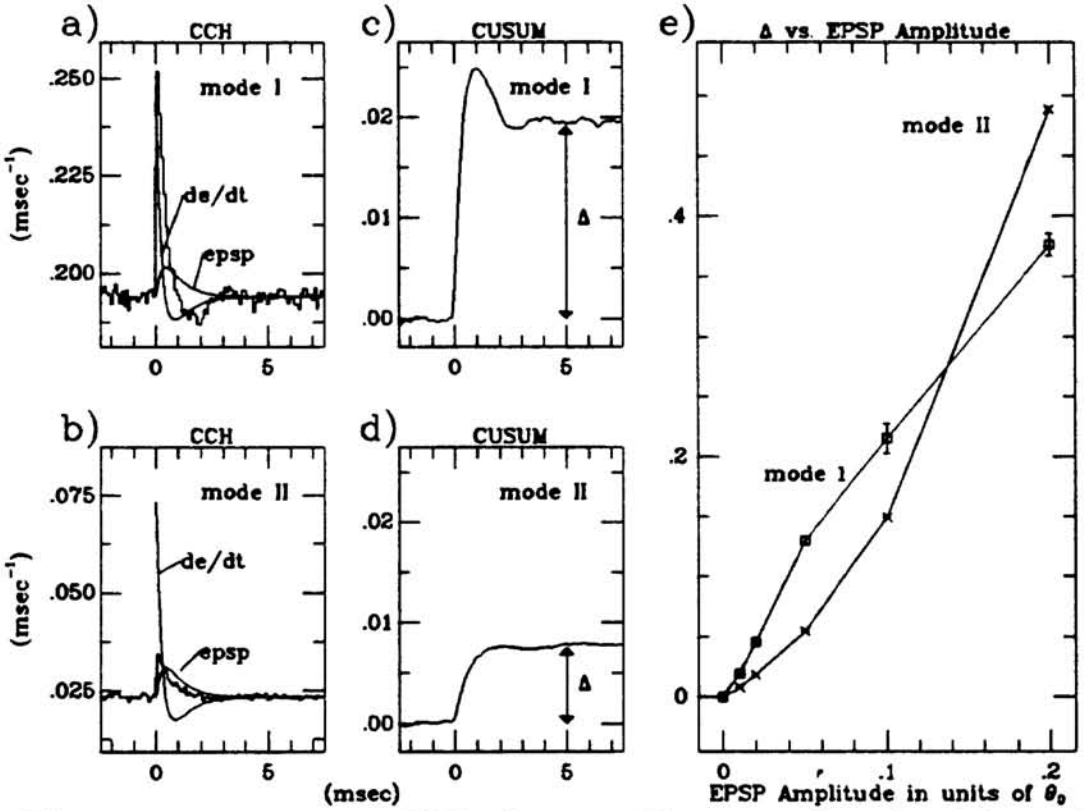

Figure 2: Response to *EPSP* for two different modes of activity. a) and b) Cross-correlogram with Poisson input source. Mode I and mode II respectively. c) and d) *CUSUM* computed from a) and b). e) Δ vs. *EPSP* amplitude for both modes of activity.

4 Analog Neuron Models

The histograms shown in Figures 2a,b may be used to compute the impulse response kernel, U, for a cell in either of the two modes of activity, simply by subtracting the baseline firing rate and normalizing to a unit impulse strength. If the cell behaves as a linear system in response to a small impulse, U may be used to compute the response of the cell to any time-varying input. In terms of U, the change in firing rate, δF, produced by an external source of Poisson-distributed impulses arriving with an instantaneous frequency $F_e(t)$ is given by

$$\delta F(t) = \int_{-\infty}^{t} U(t-t')F_e(t')T_e dt' \tag{4}$$

where, T_e is the amplitude of the incoming *EPSP's*. For the layered network used in our simulations, equation 4 may be generalized to yield an iterative relation giving the signal in one layer in terms of the signal in the previous layer.

$$\delta F_{i+1} = N \int_{-\infty}^{t} U(t-t')\delta F_i(t')T_{i+1,i}dt' \tag{5}$$

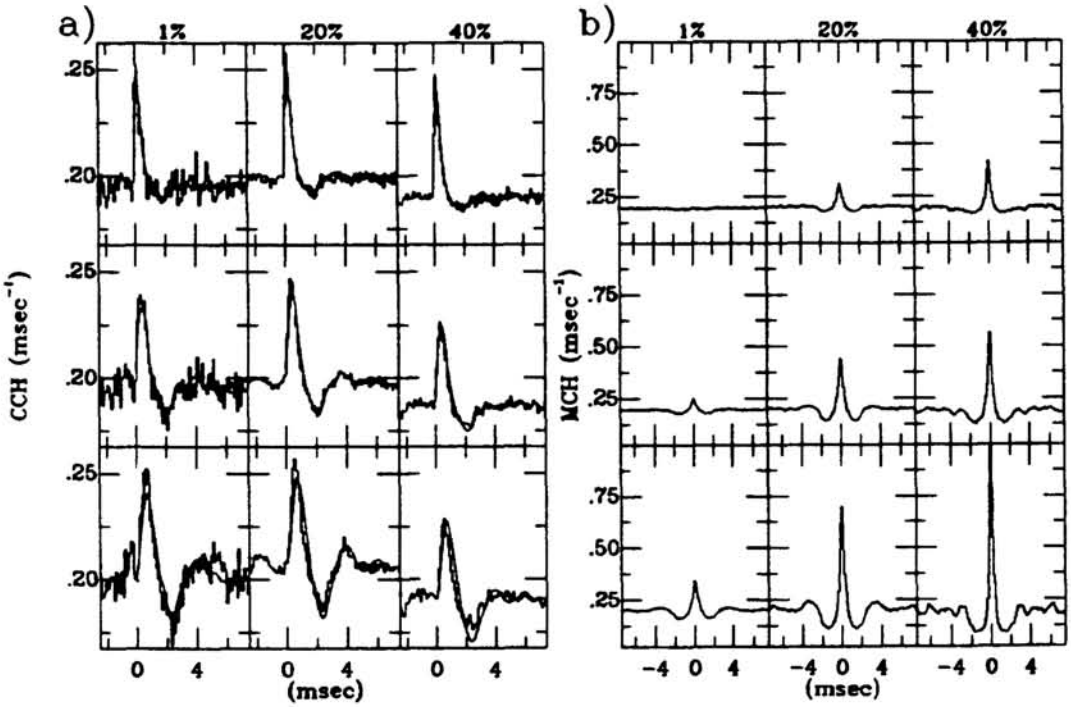

Figure 3: Signal propagation in mode I network. a) Response in first three layers due to a single impulse delivered simultaneously to all cells in the first layer. Ratio of common to independent input given by percentages at top of figure. First row corresponds to input layer. Firing synchrony does not effect signal propagation through mode I cells. Prediction of analog neuron model (solid line) gives a good description of signal propagation at all synchrony levels tested. b) Synchrony between cells in the same layer measured by MCH. Firing synchrony within a layer increases with layer depth for all initial values of the synchrony in the first layer.

where, δF_i is the change in instantaneous firing rate for cells in the i^{th} layer, $T_{i+1,i}$ is the synaptic weight between layer i and $i+1$, and N is the number of cells per layer. Equation 5 follows from an equivalent analog neuron model with a linear input-output relation. This convolution method has been proposed previously [6].

5 Effects of Firing Synchrony on Signal Propagation

A layered network was designed such that the cells in the first layer receive impulses from both common and independent sources. The ratio of the two inputs was adjusted to control the degree of firing synchrony between cells in the initial layer. Each cell in a given layer projects to all the cells in the succeeding layer with equal strength, $\frac{1}{100}\theta_0$. All simulations use 50 cells per layer.

Figure 3a shows the response of cells in the mode I state to a single impulse of strength $\frac{1}{100}\theta_0$ delivered simultaneously to all the cells in the first layer. In this and all subsequent figures, successive layers are shown from top to bottom and synchrony (defined as the fraction of common input for cells in the first layer) increases from

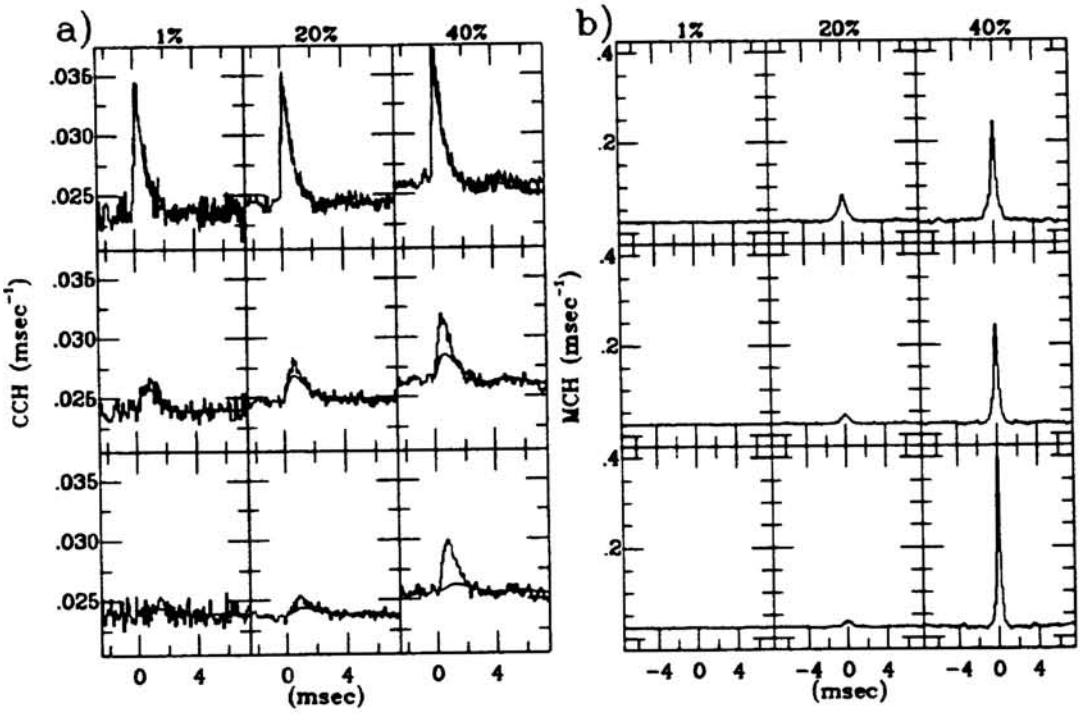

Figure 4: Signal propagation in mode II network. Same organization as fig. 3. a) At initial levels of synchrony above $\approx$ 30%, signal propagation is amplified significantly. The propagation of relatively asynchronous signals is still adequately described by the analog neuron model. b) Firing synchrony within a layer increases with layer depth for initial synchrony levels above $\approx$ 30%. Below this level synchrony within a layer decreases with layer depth.

left to right. Figure 3a shows that signals propagate through layers of interneurons with little dependence on firing synchrony. The solid line is the prediction from an equivalent analog neuron model with a linear input-output relation (eq. 5). At all levels of input synchrony, signal propagation is reasonably well approximated by the simplified model.

Firing synchrony between cells in the same layer may be measured using a mass correlogram (*MCH*). The *MCH* is defined as the auto-correlation of the population spike record, which combines the individual spike records of all cells in a given layer. Figure 3b shows that for all initial levels of synchrony produced in the input layer, the intra-layer firing synchrony increased rapidly with layer depth.

The simulations were repeated using an identical network, but with the tonic level of input reduced sufficiently to fix the cells in the mode II state (fig. 4). In contrast with the mode I case, the effect of firing synchrony is substantial. When firing is asynchronous only a weak impulse response is present in the third layer (fig. 4a, bottom left), as predicted by the analog neuron model (eq. 5). For levels of input synchrony above $\approx$ 30%, however, the response in the third layer is substantially more prominent. A similar effect occurs for synchrony within a layer. At input

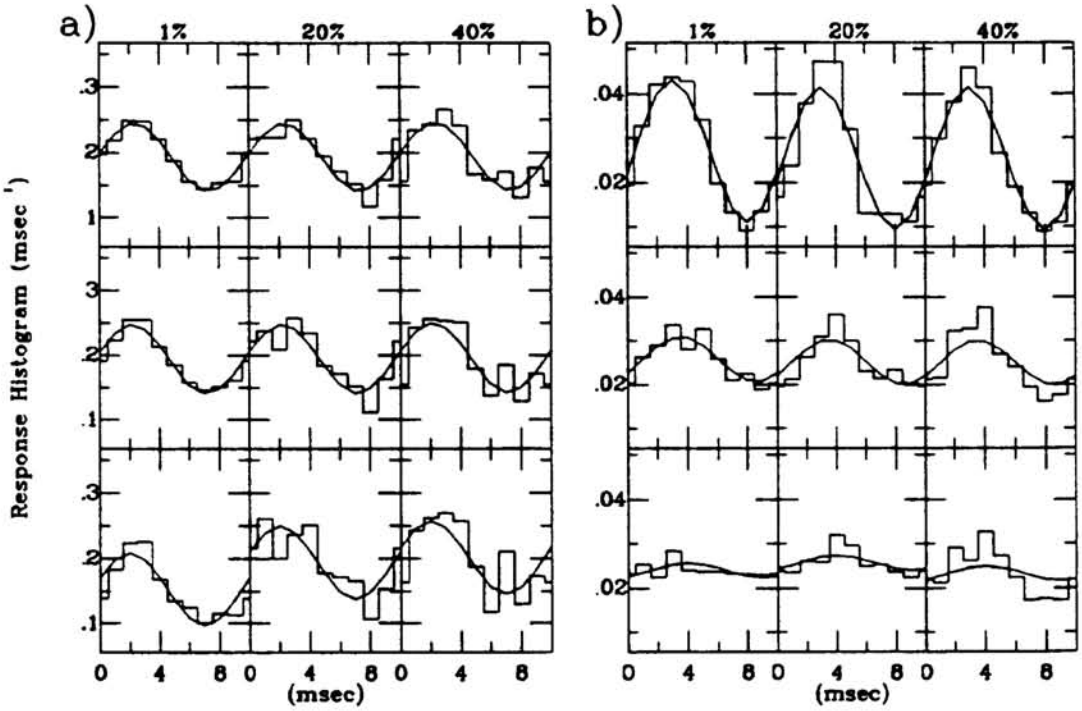

Figure 5: Propagation of sinusoidal signals. Similar organization to figs. 3,4. Top row shows modulation of input sources. a) Mode I activity. Signal propagation is not significantly influenced by the level of firing synchrony. Analog neuron model (solid line) gives reasonable prediction of signal tranmission. b) Mode II activity. At initial levels of firing synchrony above $\approx$ 30%, signal propagation is amplified. The propagation of asynchronous signals is still well described by the analog neuron model. Period of applied oscillation = 10 msec.

synchrony levels below $\approx$ 30%, firing synchrony between cells in the same layer (fig. 4b) falls off in successive layers. Above this level, however, synchrony grows rapidly from layer to layer.

To confirm that our results are not limited to the propagation of signals generated by a single impulse, oscillatory signals were produced by sinusoidally modulating the firing rates of both the common and independent input sources to the first layer (fig. 5). In the mode I state (fig. 5a), we again find that firing synchrony does not significantly alter the degree of signal penetration. The solid line shows that signal transmission is adequately described by the simplified model (eqs. 4,5). In the mode II case, however, firing synchrony is seen to have an amplifying effect on sinusoidal signals as well (fig. 5b). Although the propagation of asynchronous signals is well described by the analog neuron model, at higher levels of synchrony propagation is enhanced.

6 Discussion

It is widely accepted that biological neurons code information in their spike density or firing rate. The degree to which the firing correlations between neurons can code additional information by modulating the transmission of FM signals, depends strongly on dynamical factors. We have shown that for cells whose average membrane potential is sufficiently below the threshold for firing, spike correlations can significantly enhance the transmission of FM signals. We have also shown that the propagation of asynchronous signals is well described by analog neuron models with linear transforms. These results may be useful for understanding the role played by synchronized *SEO's* in primary visual cortex [1, 2]. Such signals may be propagated more effectively to subsequent processing areas as a consequence of their relative synchronization.

These observations may also pertain to the neural mechanisms underlying the increased levels of synchronous discharge of cerebral cortex cells observed in slow wave sleep [7]. Another relevant phenomenon is the spread of synchronous discharge from an epileptic focus; the extent to which synchronous activity is propagated through surrounding areas may be modulated by changing their level of activation through voluntary effort or changing levels of arousal. These physiological phenomena may involve mechanisms similar to those exhibited by our network model.

Acknowledgements

This work is supported by an NIH pre-doctoral training grant in molecular biophysics (grant # T32-GM 08268) and by the Office of Naval Research (contract # N 00018-89-J-1240).

References

[1] C. M. Gray, P. König, A. K. Engel, W. Singer, *Nature* **338**:334–337 (1989)

[2] R. Eckhorn, R. Bauer, W. Jordan, M. Brosch, W. Kruse, H. J. Reitboeck, *Bio. Cyber.* **60**:121–130 (1988)

[3] E. E. Fetz, B. Gustafsson, *J. Physiol.* **341**:387–410 (1983)

[4] P. A. Kirkwood, *J. Neurosci. Meth.* **1**:107–132 (1979)

[5] M. Abeles, *Local Cortical Circuits: Studies of Brain Function.* Springer, New York, Vol. **6** (1982)

[6] E. E. Fetz, *Neural Information Processing Systems* American Institute of Physics. (1988)

[7] H. Noda, W.R.Adey, *J. Neurophysiol.* **23**:672-684 (1970)